Pacific Graphics (2017)
J. Barbic, W.-C. Lin, and O. Sorkine-Hornung (Editors)

Short Paper

Robust Gas Condensation Simulation with SPH based on Heat Transfer

Taiyou Zhang[1], Jiajun Shi[1], Changbo Wang[1†], Hong Qin[2], and Chen Li[1,2]

[1]School of Computer Science and Software Engineering , East China Normal University, Shanghai, China
[2]State University of New York at Stony Brook, Stony Brook, NY 11794, USA

Abstract

Most simulation of natural phenomena in graphics are physically based, oftentimes involving heat transfer, phase transition, environmental constraints, and/or a combination of the above. At the numerical level, the particle-based schemes (e.g., smooth particle hydrodynamics (SPH)) have proved to preserve subtle details while accommodating large quantity of particles and enabling complex interaction during heat transition. In this paper, we propose a novel hybrid complementary framework to faithfully model intricate details in vapor condensation while circumventing disadvantages of the existing methods. The phase transition is governed by robust heat transfer and dynamic characteristic of condensation, so that the condensed drop is precisely simulated by way of the SPH model. We introduce the dew point to ensure faithful visual simulation, as the atmospheric pressure and the relative humidity were isolated from condensation. Moreover, we design a equivalent substitution for ambient impacts to correct the heat transfer across the boundary layer and reduce the quantity of air particles being utilized. To generate plausible high-resolution visual effects, we extend the standard height map with more physical control and construct arbitrary shape of surface via the reproduction on normal map. We demonstrate the advantages of our framework in several fluid scenes, including vapor condensation on a mirror and some more plausible contrasts.

CCS Concepts

•***Computing methodologies*** → ***Physical simulation;***

1. Introduction and Rationale

Outdoor Condensation comprises many fascinating subtle phenomena, including the motion of drops, the formation of micro-drops, the mist, etc. Therefore, the high-fidelity graphics simulation of outdoor condensation with appealing visual effects would involve a series of physical processes, including heat transfer, convection, phase transition, and motion of condensed drops, hence it remains a challenging subject in graphics research.

To date, the complicated graphical processes of condensation remain to be under-explored. The involvement of phase transition has been described in many previous literatures, such as [DM14, SSJ*14], where the process of phase transition contains latent energy, heat transfer, and various heat source. On the contrary, the air convection is generally either ignored or simplified [IUDN10], which results in spurious effects in condensation simulation.

During the interaction of heat transfer, previous works including LBM [WZW17], mesh [MK03] and SPH [SAC*99, PPLT06], usually focus on material parameters, and pay less attention to other environmental factors like the surface tension, gravity, resistance, and many other external forces. The common method to simulate air convection is generally based on mesh, which takes advantage in large scale scenery simulation or solid deformation [CKP*16], but suffers from the lack of details in micro-domain. All of these defects may cause artifacts during condensation.

In this paper, the dew point is involved in our framework to control the phase transition of water dynamically. To balance the humidity of air particles during condensation, we employ the humidity diffusion model based on SPH. We devise an equivalent substitution for ambient impacts of involved objects to ensure heat transfer between inside and outside. Air particles are decomposed into either high-participation or low-participation area, and the iterations of the latter are simplified. To achieve detailed visual effects, we employ an augmented height map to model and simulate shapes of drops at each stage. We further improve complicated surfaces by applying Rodrigues' rotation formula. The main contributions are as follows:

- A dynamic phase transition model combined with atmospheric pressure and relative humidity to describe the process of heat transfer with air underlying the dew point.
- An equivalent substitution method based on SPH to complement the heat transfer across the boundary layer.

† Corresponding Author

DOI: 10.2312/pg.20171321

- An augmented height map to achieve smooth transition in condensation and to enhance the dimension with depth information.

2. Related Work

There are common challenges in the description of heat transfer and phase transition when we try to simulate the condensation. After the drops are condensed, the tracking and trace of the shapes of drops remains a complex work.

Heat Transfer and Phase Transition. Heat transfer and phase transition are inherent physical processes in nature, which affect many interesting phenomena.

When it comes to heat transfer simulation, it's important to choose an appropriate heat conduction formula. [Tao11] introduces a second-order heat transfer formula in their SPH model, while [PPLT06] uses a first-order formula. The latter is adopted in our approach taking account of heat conservation as mentioned in [CM99]. Also, different methods are used to model phase transition. [SAC*99, CWSO13] vary viscosity with temperature to change object's phase, while [IUDN10, MGG*10] propose latent heat to simulate phase transition.

In our approach, sufficient contact between particles in different phases should be guaranteed. Yet sufficient contact brings the inevitable huge quantity of particles. To solve this problem, [IUDN10] introduces Newton's law of cooling and applies constant heat instead of air particles. [RYY*16] proposes an equivalent substitution method of air to reduce the amount of air particles. We improve the method introduced by [RYY*16] and propose our own equivalent substitution method on environmental heat transfer.

As Maréchal et al. [MGG*10] do, we introduce the dew point and furthermore propose a dynamic phase transition model to constantly adjust the dew point according to the relative humidity.

Water Drop Simulation. After condensation, condensed drops fall down along the surface affected by gravity, surface tension, friction force, etc.

There are several approaches to simulate water drops till now. [IUDN10] uses SPH to simulate drops, but pays no attention on the shapes of drops; [WMT07] models drops by setting different height using shallow wave equation. But compared with SPH, their methods are poor at physical accuracy; [CWSO13] adopts volumetric meshes to model drops and achieves plausible results, which suffers from efficiency problem during topological changes. [TWGT10, ZR16] propose mesh-based methods to simulate water drops, but they may lack robustness in general fluid simulation. Taking consideration of physical accuracy and performance, we combine SPH with a height map as Chen et al. [CCW13] do. We perform physical-based simulation with SPH, and deal with the behaviors of drops by height map.

When simulating the shapes of drops, [WMT07] applies virtual surface to model contact angle and to affect the shapes of drops. While we adopt a formula introduced in [CCW13] which affects shapes according to mass of the particles.

Although [CCW13] achieves plausible results, it takes no consideration of physical accuracy in its drop direction selection process. The velocity computed by SPH only decides the size of the force while direction is decided by subjective judgment. To overcome this deficiency, we introduce air pressure model in our approach.

3. The Condensation Simulation Overview

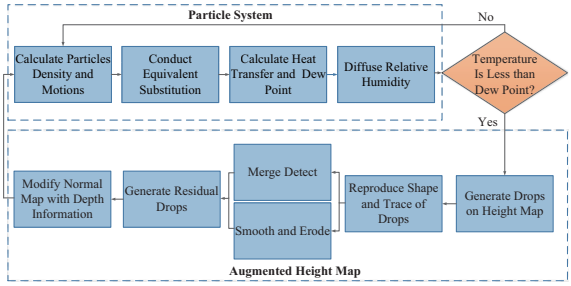

Figure 1: *Flow diagram of our framework in this paper.*

Our system can be divided in two parts: in the particle system part, we control the size of drops by a relative humidity model, and introduce dew point to dominate the process of phase transition dynamically (see Section 4). We also devise a equivalent substitution to tradeoff the balance between physical accuracy and the computational cost (see Section 5); in the augmented height map part, we improve the classic height map method with vapor effects as an interim period, more physical constraints in shape and trace of drops and depth information to handle more complex terrains (see Section 6). Fig. 1 shows the main process of our system.

4. Dynamic Phase Transition in Condensation with Convection

Condensation occurs when the vapor is cooled to its saturation limit and the relative humidity in the air phase reaches its maximum threshold. The air around the interface should be concerned with the phenomenon. According to thermal expansion and contraction, the density of air changes, thus causing the convection which accelerates the heat transfer.

In addition, condensation occurs more frequently on the surface of a bottle with water rather than an empty one, which means that previous methods ignored some crucial factors. In this section, we combine the convection, atmospheric pressure, relative humidity and dew point to model the dynamic phase transition.

4.1. Air Convection based on Thermal Difference

Due to volume shrinkage, the air with different temperatures would be distinct in their density properties to some extent. The pressure based on density would push the cooler air down and lift the hotter air up. This motion involves the heat transfer and the distribution of condensed drops. As in [DM14], the formula for density modification is as follow:

$$\rho_0(T, \sigma_\rho) = \frac{\rho_0}{1.0 + T \cdot \sigma_\rho}, \tag{1}$$

where ρ_0 denotes the rest density of air, σ_ρ is a constant and set to 0.005, T denotes the temperature.

This modification could divide the air with different temperature theoretically, but it fails when the mixed air is under force equilibrium initially, for the temperature in Eq. 1 is the secondary factor in force calculation. Changing the density with Eq. 1 cannot break this unwanted balance in which hot particles may be blocked by surrounding cold particles. A pure force derived from temperature is introduced to handle this problem as a supply:

$$\mathbf{f} = \frac{\sigma_f}{T_{\max} - T_i}\mathbf{v}_{up}, \tag{2}$$

where $\mathbf{f}$ refers to the force related to temperature, σ_f refers to the float constant, T_{max} is the highest temperature allowed, and $\mathbf{v}_{up}$ is the unit velocity upward.

Combined Eq. 1 with Eq. 2, the air would be divided into two parts. The hotter one stays upper, while the cooler one moves down.

4.2. Relative Humidity Diffusion Formula

The prerequisite of condensation is that the air which is under the saturated atmospheric pressure contains a certain amount of water at the proper temperature. The relative humidity is the physical property which measures the amount of water contained in the air molecules, and plays a vital role in determining the size of the condensed drops. Due to the strong convection, the humidity exchange should be taken into account.

According to Fick's Law [Fic95], in one-dimension, the flux goes from high-concentration regions to low-concentration regions, with a magnitude that is proportional to the concentration gradient:

$$J = -D\frac{\partial \phi}{\partial x}, \tag{3}$$

where J refers to the diffusion flux, D refers to the diffusion coefficient which is determined by the properties of the material itself, the nature of the diffusion intermediary and their ambient atmospheric pressure, temperature, etc. ϕ refers to the concentration.

Derived from Eq. 3 and the law of conservation of mass, the formula how diffusion causes the concentration to change with time is:

$$\frac{\partial \phi}{\partial t} = -\frac{\partial}{\partial x}J = \frac{\partial}{\partial x}\left(D\frac{\partial \phi}{\partial x}\right) = D\frac{\partial^2 \phi}{\partial x^2}, \tag{4}$$

In two-dimension, the diffusion model of relative humidity is:

$$\frac{\partial \phi}{\partial t} = D\nabla^2\phi. \tag{5}$$

4.3. Dynamic Phase Transition governed by Dew Point

Dew point is defined as the temperature which the air is cooled to saturation temperature when humidity and pressure stay constant. During condensation process, the dew point changes dynamically. In discrete system, we acquire the relation between the pressure and the temperature via Clausius-Clapeyron [Cla60] formulation:

$$\frac{dP}{dT} = \frac{L}{T\Delta V} = \frac{\Delta s}{\Delta V}, \tag{6}$$

where P denotes atmospheric pressure, T denotes the phase transition temperature, L denotes the latent energy of unit mass, V denotes the volume of unit mass.

Under standard atmospheric and normal temperature, the Clausius-Clapeyron equation for the corresponding water vapor is:

$$\frac{dP_s}{dT} = \frac{L_v(T)P_s}{R_v T^2}, \tag{7}$$

where P_s refers to the saturated vapor pressure, L_v refers to the unit modulus of water vaporization latent heat, R_v refers to the gas constant of vapor.

According to Eq. 7, we can see that P_s is a function that depends on T. On the basis of Eq. 7, August-Roche-Magnus raised an approximate estimation:

$$T_{dp} = \frac{c\gamma(T,RH)}{b-\gamma(T,RH)}, \tag{8}$$

$$\gamma(T,RH) = \ln\left(\frac{RH}{100}\right) + \frac{bT}{c+T}, \tag{9}$$

where RH denotes the relative humidity, T_{dp} denotes the dew point. b and c in Eq. 9 are user defined constants. In this paper, we set b = 17.67, c = 243.5°C as [Bol80].

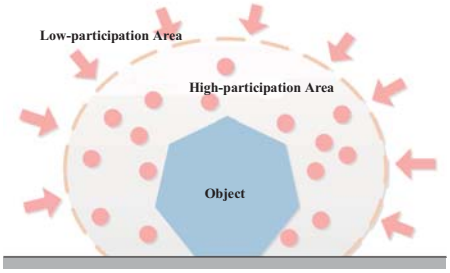

Figure 2: *The equivalent substitution for ambient air particles. The outside boundary denotes the boundary between the high-participation and low-participation area.*

5. SPH-based Heat Transfer Simulation

After the analysis of dynamic phase transition, we dicretize the theory above into SPH model. While scenarios involve heat transfer, the environmental heat source is usually underestimated. A common treatment is to set environmental temperature as a constant or a function of surface area [IUDN10]. In micro-phenomena, however, subtle changes would have a huge impact on final results.

5.1. Equivalent Substitution for Environmental Factors

To tradeoff the balance between physical accuracy and efficiency, we divide the experimental scenes into two parts: the high-participation area and the low-participation area, as shown in Fig. 2. Since we need to capture the details, sufficient SPH particles are well distributed in high-participation area, and the behavior of the

air particles in low-participation area can be simplified to accelerate the entire animation.

According to [RYY*16], disregard of the influence on outside ambient domain may cause particle deficiency, which would result in erroneous calculation of properties. We correct the air convection based on two common hypothesis. Since the details in small scale have significant influence on final effect, we weaken the initial constraint in [RYY*16] and derive the first hypothesis: the air particles in low-participation area are ideal distributed.

Since a temperature jump hardly occurs in a short period of time due to the high convection of ambient air, our second hypothesis is that the ambient air temperature is set to environmental temperature T_{env} with a small amplitude.

In the second-order form of heat transfer equation which is commonly used in SPH systems, calculation error will occur if the positions of two particles with different temperatures coincide, causing singularity [CM99]. We adopt the method in [CR99], using the SPH mapping method to reduce the original second-order form to the first-order form:

$$\frac{\partial T_i}{\partial t} = c_d \sum_j m_j \frac{(T_j - T_i)}{\rho_j} \frac{4\rho_i}{\rho_i + \rho_j} \frac{(\mathbf{r}_i - \mathbf{r}_j) \cdot \nabla W(\mathbf{r}_i - \mathbf{r}_j, h)}{|\mathbf{r}_i - \mathbf{r}_j|^2 + 0.01h^2}. \tag{10}$$

where T_s denotes the temperature of particle s, t denotes the time, and c_d denotes the thermal conductivity of material.

To prevent adiabatic state which makes hot and cold air particles separate and weakens the air convection, we need to keep heat exchange between inner system and ambient air. Refer to [CM99] and on the basis of Eq. 10, we follow [RYY*16] and create a virtual particle for each air particle at the boundary between high-participation and low-participation area. We substitute the ambient air in the low-participation area with virtual larger particles. The equivalent substitution for environment heat transfer is shown as:

$$\begin{aligned} \frac{\partial \bar{T}_i}{\partial t} = {} & c_d \sum_j m_j \frac{(T_j - T_i)}{\rho_j} \frac{4\rho_i}{\rho_i + \rho_j} \frac{(\mathbf{r}_i - \mathbf{r}_j) \cdot \nabla W(\mathbf{r}_i - \mathbf{r}_j, h)}{|\mathbf{r}_i - \mathbf{r}_j|^2 + 0.01h^2} \\ & + \bar{c}_d m_k \frac{(T_k - T_i)}{\rho_k} \frac{4\rho_i}{\rho_i + \rho_k} \frac{(\mathbf{r}_i - \mathbf{r}_k) \cdot \nabla W(\mathbf{r}_i - \mathbf{r}_k, h)}{|\mathbf{r}_i - \mathbf{r}_k|^2 + 0.01h^2}, \end{aligned} \tag{11}$$

where the index k refers to the virtual particle, $\bar{c}_d$ is the thermal conductivity between air particle and visual particle.

5.2. Humidity Diffusion Model based on SPH

Combined with Eq. 5, the humidity diffusion model in SPH is derived as:

$$\frac{\partial RH_i}{\partial t} = k_{diff} \sum_j m_j \frac{(RH_j - RH_i)}{\rho_j} \nabla^2 W(\mathbf{r}_i - \mathbf{r}_j, h), \tag{12}$$

where RH refers to relative humidity.

A drop particle would be added just at the position where condensation occurs. Since the mass of the drops is calculated from the relative humidity variation of the air particles, the local humidity difference would let the surrounding air particles exchange humidity properties via the humidity diffusion model after condensation.

Since the air particles rarely leave the high-participation area after the solid reaction, and then turn back to the secondary heat exchange with the solid and the condensation reaction occurs, the relative humidity properties do not require additional operations for the ambient humidity change.

6. Drop Simulation with Augmented Height Map

Algorithm 1 Animation of drops on the surface

```
while animating do
    add vapor on height map (See Section 6.1)
    for all Height(x,y) > threshold do
        clear vapor around (x,y) and form a drop
    for all liquid particle i do
        add air pressure and calculate resistance via Eq. 13
        if LeaveResidual(pr(τ_i, Δt, τ_max))) == true then
            create a new liquid particle i'
        if m_i · g == f_resist then
            shape i
        update height and ID map
    detect collision and merge drops using ID map
    smoothing and erosion
```

We follow the works in [CCW13] and propose an augmented height map method to simulate the motion of drops on surface. The major procedure is shown in Algorithm 1. We focus on our improvements as shown below:

- We apply vapor effects as an interim period to achieve smooth transition in condensation.
- We add more physical constraints and weaken random impacts in the process of shaping and tracing drops.
- We introduce depth information into surface rendering to handle more complex terrains.

6.1. Improved Drop Formation with Vapor Effect

At the moment of condensation, the usual method adds a new particle immediately, and there would be an instant change between the two frames which is like a rain hit more than condensation. After refining the condensation process, there are huge amounts of micro-scale drops integrated together which seem like vapor. In the continuous reaction, the small particles of drops continue to receive the humidity from external air, and gather together into visible drops.

There would be too many particles if we use SPH to achieve the initial micro-scale particles. Thus we adopt the height map to realize the vapor effect. The height of the grid increases according to the mass of condensed particle where condensation occurs, and the height of surrounding meshes are interpolated via the kernel function. When the height of a mesh grows bigger than a user-defined *threshold*, vapor nearby would cluster and form a drop.

6.2. Shape and Trace of Drops

For static drops, simulation in large scale would form monotonous shapes. In order to achieve the diversity of drops, [CCW13] adopts composite random processes to convert individual drops into drop

Table 1: *Timings of the different parts of the simulation.*

Height Map Resolution		256^2	512^2
100000 particles	Part A(ms)	36	38
	Part B(ms)	36	37
	Part C(ms)	3	12
200000 particles	Part A(ms)	72	72
	Part B(ms)	71	73
	Part C(ms)	3	12

segments. To make this process more plausible, we add a mass constraint to decide how many segments a drop should be divided into. Drops with larger mass tend to form more complicated shapes. We calculate the radius of a drop according to its mass using the method in [CCW13], and the drop is divided into several segments, which equals to the integer part of the square root of its radius.

In our method, each drop is mapped by a single particle. After condensation, there is no velocity difference between drop and surface since viscosity force remains zero, and surface tension cannot be calculated by only one liquid particle. So we introduce the atmospheric resistance and affinity force as supplements to the surface tension to affect the motion of drops. The equation is written as:

$$\mathbf{f}_{resist} = \sum_i \mu_i \times (P \cdot S), \tag{13}$$

where μ_i denotes the resistance of the grid, which is decided by the properties of solid, P denotes the atmospheric pressure, S denotes the the area drop covered. In our system, μ_i is randomly set for each grid within [0,1].

6.3. Dimension Enhancement with Depth Information

After the analysis of drop simulation on height map, we improve the surface with depth information. The method proposed in [CCW13] can only handle 2D scenes, which limits its adoption. To extend the usage of our augmented height map, we add terrain effects on the grids. We change the normal map derived from the height map and combine ir with the Fresnel effect and skybox.

Considering a scene with different slopes, the normal map from height map should be rotated to fit the slope on surface. The rotation matrix is solved reversely by initial normal vector and the new normal vector of the slope. The new normal map can be calculated by multiplying the normal map and the rotation matrix. The method to solve rotation matrix is called Rodrigues' rotation formula:

$$\mathbf{v}_{rot} = \mathbf{v}\cos\theta + (\mathbf{k}\times\mathbf{v})\sin\theta + \mathbf{k}(\mathbf{k}\cdot\mathbf{v})(1-\cos\theta), \tag{14}$$

where $\mathbf{v}$ and $\mathbf{v}_{rot}$ denotes the initial normal vector and rotated normal vector, $\mathbf{k}$ denotes the unit vector of rotation axis, and θ denotes the intersection angle between $\mathbf{v}$ and $\mathbf{v}_{rot}$.

7. Implementation and Experimental Results

Our experiments are performed on an Intel(R) Core(TM) i5-4590 CPU at 3.30 GHz quad core with 8 GB RAM and NVIDIA GeForce GTX960. We implemented our system with C++ and GLSL. The CUDA version applied is 7.5.

Table 1 shows the timings of three parts of the simulation. Part A denotes general SPH framework simulated on GPU, including computation of humidity diffusion and equivalent substitution. Part B denotes external particle computation on CPU like shape, trace, residual, merging of drops and computation of dew point. Part C denotes computation of height map, updating height map and computation of ID map on CPU. Higher height map resolution results in more computation costs on height map (Part C), while the number of particles mainly influences the costs of Part A and Part B which are more related to particle system.

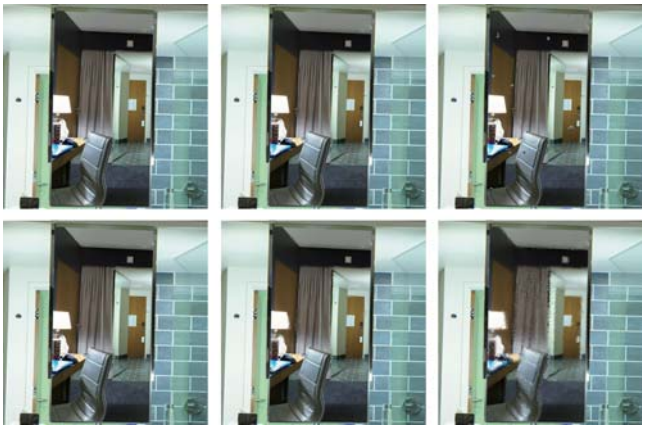

Figure 3: *Comparison of simulation on the mirror with (below) and without (upper) vapor effect.*

Fig. 3 shows the process of condensation on a mirror. The upper three figures show the effect without vapor effect, they seem more like rain drops than condensation drops. However, condensation is slow and gradual in reality. As shown in the three figures below, the mirror is first covered with condensed fine mists. With condensation goes on, the fine mists gather together and merge into small drops. In our approach, drops are formed by continuous aggregation of fine mists instead of appearing suddenly, which is closer to the reality.

Fig. 4 illustrates the dynamic phase transition in our condensation model. We choose the relative humidity as the variable and keep others constant. With the impact of higher humidity, there are much more condensed drops on the bottom of the Fig. 4, and condensation occurs much earlier.

Fig. 5 shows the difference between the cohesive method [CCW13] and our method. In cohesive method, the direction of velocity is determined by water cohesive force and the affinity of a mesh. When the neighbor grids of a moving drop lack water, the random-set affinity of grid would force the drop flow down straight with continuous wriggle, while ours shows more vivid effect.

In this paper, we devise the augmented height map with depth information to enhance dimension. By comparing the models in Fig. 6, we pay attention on the curves which reflect and refract in continuum without any artifacts. The cylinder and sphere model show that arbitrary curvature of surface are both well simulated.

8. Conclusion

This paper has proposed a new physical-based framework to simulate outdoor condensation phenomena combined with the dynamic phase transition model, the humidity diffusion model, the equivalent substitution method and the augmented height map. In the future, We would like to implement Part B and C in Table 1 on GPU with CUDA, and enable our current height map method to preserve volume and surface property to avoid probable artifacts.

Acknowledgements

This paper is partially supported by Natural Science Foundation of China under Grants 61532002 and 61672237, National High-tech R&D Program of China (863 Program) under Grant 2015AA016404.

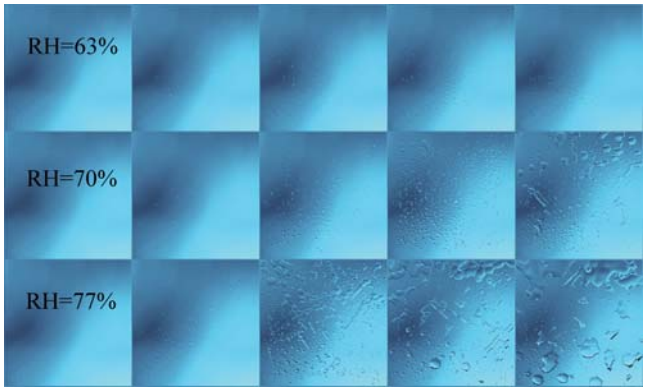

Figure 4: *Air particles with different relative humidity are forced to interact with the window, while each row keeps the same humidity. The frames of each column are 200, 300, 400, 500 and 600.*

Figure 5: *Comparison between cohesive method (left) [CCW13] and our method (right).*

Figure 6: *Three different models with a PG logo in the center.*

References

[Bol80] BOLTON D.: The computation of equivalent potential temperature. *Monthly weather review 108*, 7 (1980), 1046–1053. 3

[CCW13] CHEN K. C., CHEN P. S., WONG S. K.: A heuristic approach to the simulation of water drops and flows on glass panes. *Computers & Graphics 37*, 8 (2013), 963–973. 2, 4, 5, 6

[CKP*16] CHERN A., KNÖPPEL F., PINKALL U., SCHRÖDER P., WEISSMANN S.: Schrödinger's smoke. *ACM Transactions on Graphics (TOG) 35*, 4 (2016), 77. 1

[Cla60] CLAUSIUS R.: *On the Motive Power of Heat, and on the Laws which Can be Deduced from it for the Theory of Heat*. Annalen der Physik. Dover, 1960. 3

[CM99] CLEARY P. W., MONAGHAN J. J.: Conduction modelling using smoothed particle hydrodynamics. *Journal of Computational Physics 148*, 1 (1999), 227–264. 2, 4

[CR99] CUMMINS S. J., RUDMAN M.: An sph projection method. *Journal of computational physics 152*, 2 (1999), 584–607. 4

[CWSO13] CLAUSEN P., WICKE M., SHEWCHUK J. R., O'BRIEN J. F.: Simulating liquids and solid-liquid interactions with lagrangian meshes. *ACM Transactions on Graphics (TOG) 32*, 2 (2013), 17. 2

[DM14] DOMARADZKI J., MARTYN T.: Improved particle-based ice melting simulation with sph air model. 1, 2

[Fic95] FICK A.: On liquid diffusion. *Journal of Membrane Science 100*, 1 (1995), 33–38. 3

[IUDN10] IWASAKI K., UCHIDA H., DOBASHI Y., NISHITA T.: Fast particle-based visual simulation of ice melting. In *Computer Graphics Forum* (2010), vol. 29, Wiley Online Library, pp. 2215–2223. 1, 2, 3

[MGG*10] MARÉCHAL N., GUÉRIN E., GALIN E., MÉRILLOU S., MÉRILLOU N.: Heat transfer simulation for modeling realistic winter sceneries. In *Computer Graphics Forum* (2010), vol. 29, Wiley Online Library, pp. 449–458. 2

[MK03] MELEK Z., KEYSER J.: Interactive simulation of burning objects. In *Computer Graphics and Applications, 2003. Proceedings. 11th Pacific Conference on* (2003), IEEE, pp. 462–466. 1

[PPLT06] PAIVA A., PETRONETTO F., LEWINER T., TAVARES G.: Particle-based non-newtonian fluid animation for melting objects. In *Computer Graphics and Image Processing, 2006. SIBGRAPI'06. 19th Brazilian Symposium on* (2006), IEEE, pp. 78–85. 1, 2

[RYY*16] REN B., YAN X., YANG T., LI C.-F., LIN M. C., HU S.-M.: Fast sph simulation for gaseous fluids. *The Visual Computer 32*, 4 (2016), 523–534. 2, 4

[SAC*99] STORA D., AGLIATI P. O., CANI M. P., NEYRET F., GASCUEL J. D.: Animating lava flows. In *Conference on Graphics Interface* (1999), pp. 203–210. 1, 2

[SSJ*14] STOMAKHIN A., SCHROEDER C., JIANG C., CHAI L., TERAN J., SELLE A.: Augmented mpm for phase-change and varied materials. *ACM Transactions on Graphics (TOG) 33*, 4 (2014), 138. 1

[Tao11] TAO J.: The first order symmetric sph method for transient heat conduction problems. *Physics 60*, 9 (2011), 090206–601. 2

[TWGT10] THÜREY N., WOJTAN C., GROSS M., TURK G.: A multiscale approach to mesh-based surface tension flows. In *ACM Transactions on Graphics (TOG)* (2010), vol. 29, ACM, p. 48. 2

[WMT07] WANG H., MILLER G., TURK G.: Solving general shallow wave equations on surfaces. In *ACM Siggraph/eurographics Symposium on Computer Animation* (2007), pp. 229–238. 2

[WZW17] WU W., ZHANG S., WANG S.: A novel lattice boltzmann model for the solid–liquid phase change with the convection heat transfer in the porous media. *International Journal of Heat and Mass Transfer 104* (2017), 675–687. 1

[ZR16] ZUBRZYCKI M., RACZKOWSKI J.: Surface tension and wettability modeling for flowing liquids. In *Computer Graphics, Imaging and Visualization (CGiV), 2016 13th International Conference on* (2016), IEEE, pp. 12–17. 2